Chinese Chemical Letters 33 (2022) 5051–5055

Contents lists available at ScienceDirect

Chinese Chemical Letters

journal homepage: www.elsevier.com/locate/cclet

Dual microenvironmental parameter-responsive lysosome-targeting carbon dots for the high contrast discrimination of a broad spectrum of cancer cells

Yue Xiao, Xiaohui Yin, Pengjuan Sun, Yuanqiang Sun*, Lingbo Qu, Zhaohui Li*

College of Chemistry, Institute of Analytical Chemistry for Life Science, Henan Joint International Research Laboratory of Green Construction of Functional Molecules and Their Bioanalytical Applications, Zhengzhou University, Zhengzhou 450001, China

ARTICLE INFO

Article history:
Received 23 December 2021
Revised 16 March 2022
Accepted 30 March 2022
Available online 2 April 2022

Keywords:
Carbon dots
Multiple microenvironmental parameters
Lysosome-targeting
High contrast imaging
Cancer diagnosis

ABSTRACT

The development of new carbon dots (CDs) for fluorescence-based cancer diagnosis has recently attracted extensive attention. Diagnosis methods based on ligand-receptor fluorescence suffer from the heterogeneity of receptor expression. Changes in the microenvironments of cancer cells provide opportunities for accurate and broad-spectrum cancer diagnosis. The lysosomes in cancer cells have lower polarity and higher viscosity than normal cells. Based on these two key microenvironmental parameters, dual-responsive CDs with inherent lysosome-targeting ability were synthesized *via* one-step hydrothermal treatment. The CDs exhibit many advantageous properties including facile synthesis, good water solubility, pH-independent emission, excellent photostability, good biocompatibility, and wash-free imaging ability. The CDs were successfully employed in the fluorescence-based discrimination of a broad spectrum of cancer cells from normal cells with high contrast. The CDs are promising candidates for use in the field of cancer diagnosis.

As a highly invasive disease with a high mortality rate, cancer seriously threatens human health [1]. Much attention has been devoted to developing new tools for acute cancer diagnosis [2]. At present, a variety of clinical detection methods for cancer diagnosis and treatment are widely employed, such as X-ray computed tomography, magnetic resonance imaging, and ultrasound [3,4]. However, these techniques have some shortcomings, including low specificity, low signal-to-noise ratio, radiation overdose, and high cost [5]. In contrast, fluorescence imaging has attracted increasing attention in recent years due to its high spatiotemporal resolution, cost effectiveness, and lack of radiation [4,6-8].

Carbon dots (CDs) [9–11], zero-dimensional nanomaterials, have been widely used in the field of fluorescent sensing and bioimaging due to their good biocompatibility [12], low toxicity [13], excellent photostability [14–16], easy synthesis and purification [17], and low cost [18]. Many pioneering works on CDs-based fluorescent probes for cancer diagnosis have been reported in recent years. For example, fluorescent CDs for cancer diagnosis were developed by taking advantage of the altered permeability of the cancer membrane or the typical aerobic glycolysis process of cancer cells [19,20]. To date, the most common strategy for cancer diagnosis by using CDs is based on the interactions between ligand-modified CDs and the surface receptor of the cancer cells [21,22], which is less effective when considering the fact that cancer is a highly heterogeneous disease associated with abnormal mutations. As is well known, the expressions of cancer-related receptors differ both between patients and within the same patient [23]. Therefore, novel design strategies for fluorescence-based high contrast discrimination of cancer are highly needed.

Cancer cells are characterized by the expressions of cell surface receptors and nucleic acids along with the characteristics of the intracellular microenvironment, including polarity, viscosity, pH, and hypoxia [24,25]. Therefore, intracellular microenvironments can serve as effective cancer makers. However, the design of microenvironment-based CDs for cancer diagnosis faces several challenges. First, CDs that are responsive to a single microenvironmental parameter (*e.g.*, pH-responsive CDs) may suffer from low accuracy. CDs that are responsive to multiple microenvironmental parameters are highly required to obtain high fluorescence contrast [26]. Second, the microenvironments of various organelles in cancer cells (*e.g.*, lysosome, mitochondria, and endoplasmic reticulum) are highly different [27,28]. To achieve high accuracy, microenvironment-responsive CDs should also have inherent organelle-targeting ability.

Lysosomes play critical roles in cancer development and metastasis; thus, lysosomes have become a target for effective cancer di-

* Corresponding authors.
E-mail addresses: sunyq@zzu.edu.cn (Y. Sun), zhaohui.li@zzu.edu.cn (Z. Li).

https://doi.org/10.1016/j.cclet.2022.03.109
1001-8417/

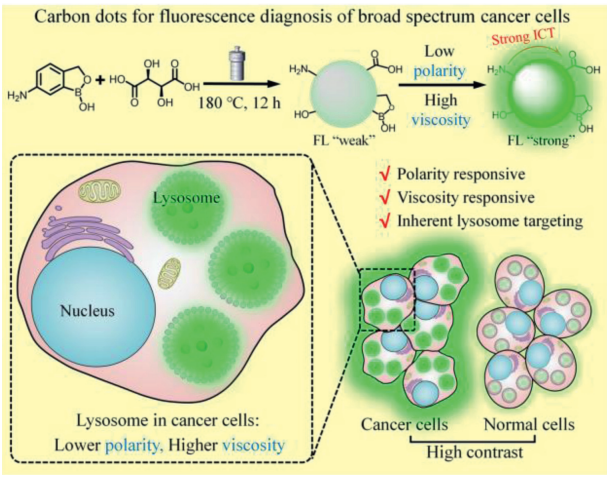

Scheme 1. Synthetic route and sensing model of the CDs for lysosome targeting and distinguishing between cancer cells and normal cells.

agnosis and treatment [29]. Recent studies have revealed that the lysosomes in cancer cells have lower polarity [30] and higher viscosity [31] than those in normal cells. These differences have a great potential to serve as the basis for the design of dual stimuli-responsive CDs for precise cancer diagnosis. Herein in this work, polarity- and viscosity-responsive CDs co-doped with B and N were synthesized *via* one-step hydrothermal treatment, which possess inherent lysosome-targeting ability (Scheme 1). Due to the presence of electron-donating amino groups and electron-withdrawing boronic acid as well as carboxylic acid groups, the CDs exhibited effective intramolecular charge transfer (ICT) under excitation, thereby endowing the CDs with good responsiveness to polarity and viscosity [32–34]. The CDs showed weak fluorescence in high-polarity and low-viscosity solvents, while exhibited strong fluorescence in solvents with low polarity and high viscosity. By taking advantage of the low-polarity, high-viscosity microenvironments of cancerous lysosomes, the CDs were successfully employed in the fluorescence-based discrimination of cancer cells from normal cells with high contrast. Moreover, the CDs-based nanoprobes exhibit many advantages, including facile synthesis, good water solubility, pH-independent emission, good biocompatibility, excellent photostability and wash-free imaging ability, which are promising candidates for application in the field of cancer diagnosis and biological studies.

The preparation of CDs with desirable optical and biological properties could be achieved by carefully choosing the precursors. For accurate and specific cancer diagnosis through lysosome imaging, the CDs should selectively stain lysosomes and respond to low polarity and high viscosity. Therefore, the precursors and CDs should meet the following requirements: (1) The precursors should be rich in amino groups to endow the as-prepared CDs with intrinsic lysosome-targeting ability since the lysosomes are the most acidic organelles, and lipophilic amines are enriched in lysosomes by over 100 times compared to that in other organelles [28]; (2) the CDs should contain electron-donating groups (*e.g.*, $-NH_2$ and –OH) and electron-withdrawing groups (*e.g.*, carbonyl and boronic groups) to form effective ICT systems, thereby making the CDs sensitive to the changes in polarity and viscosity upon light excitation [32]; and (3) the precursors should contain multiple functional groups (*e.g.*, carboxylic and hydroxyl groups) that can undergo condensation, polymerization, and carbonization to form carbon nuclei and fluorescent centers [35].

Therefore, 6-aminobenzo[*c*][1,2]oxaborol-1(3*H*)-ol was selected as the precursor due to its aromatic amino groups and electron-withdrawing boronic acid groups. L(+)-tartaric acid was selected because it contains multiple carboxylic and hydroxyl groups [36]. The carboxylic groups of L(+)-tartaric acid are expected to undergo Friedel–Crafts reaction with 6-aminobenzo[*c*][1,2]oxaborol-1(3*H*)-ol to form the ketone intermediate, which reacts to form carbon nuclei and fluorescent centers attribute to the presence of carboxyl and hydroxyl groups. Based on this design, dual polarity- and viscosity-responsive fluorescent CDs with intrinsic lysosome-targeting ability for cancer diagnosis were obtained.

The B/N-co-doped CDs were hydrothermally synthesized from 6-aminobenzo[*c*][1,2]oxaborol-1(3*H*)-ol and L(+)-tartaric acid at 180 °C for 12 h. The morphology was characterized by transmission electron microscopy (TEM; Fig. 1a). The CDs were spherical with diameters ranging from 4 nm to 10.5 nm (average diameter = 7.32 ± 0.3 nm). As can be seen in Fig. 1b, the X-ray diffraction (XRD) pattern shows a broad (002) diffraction peak at around

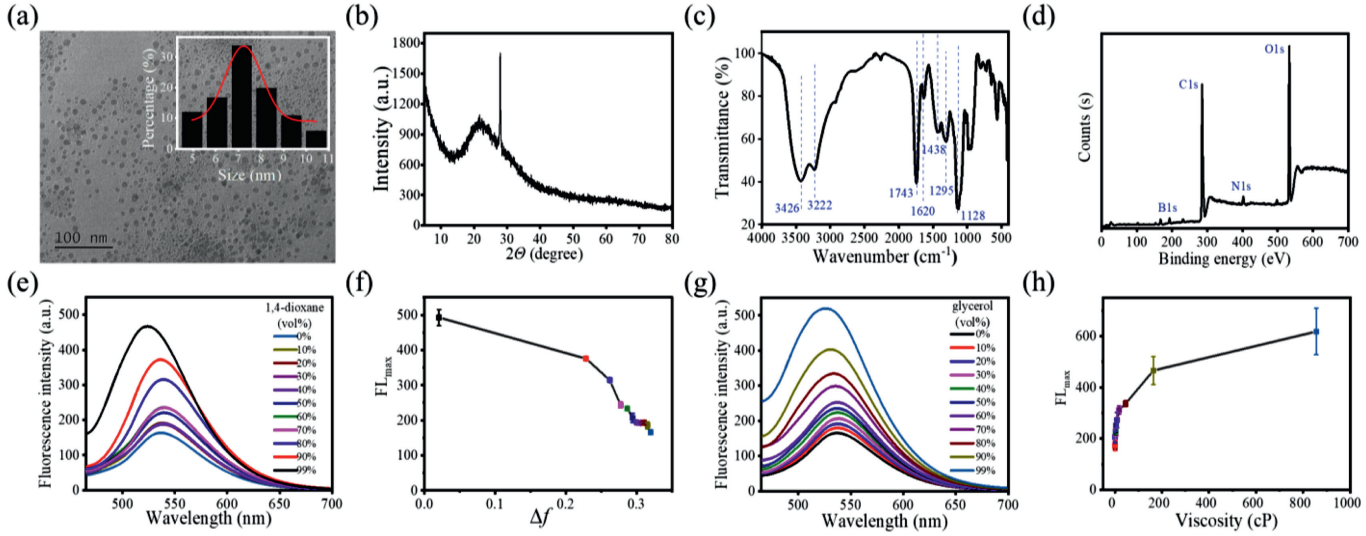

Fig. 1. Characterization of the CDs: (a) TEM image (inset: the size distribution histogram; scale bar: 100 nm), (b) XRD spectrum, (c) FTIR spectrum, and (d) XPS spectrum. Optical properties of the CDs: (e) Fluorescence spectra of the CDs in different 1,4-dioxane/H_2O solvent mixtures with 1,4-dioxane contents ranging from 0% to 99%. (f) Relationship between the maximum fluorescence intensity and the polarity index. (g) Fluorescence spectra of the CDs in different glycerol/H_2O solvent mixtures with glycerol contents ranging from 0% to 99%. (h) Relationship between the maximum fluorescence intensity and viscosity.

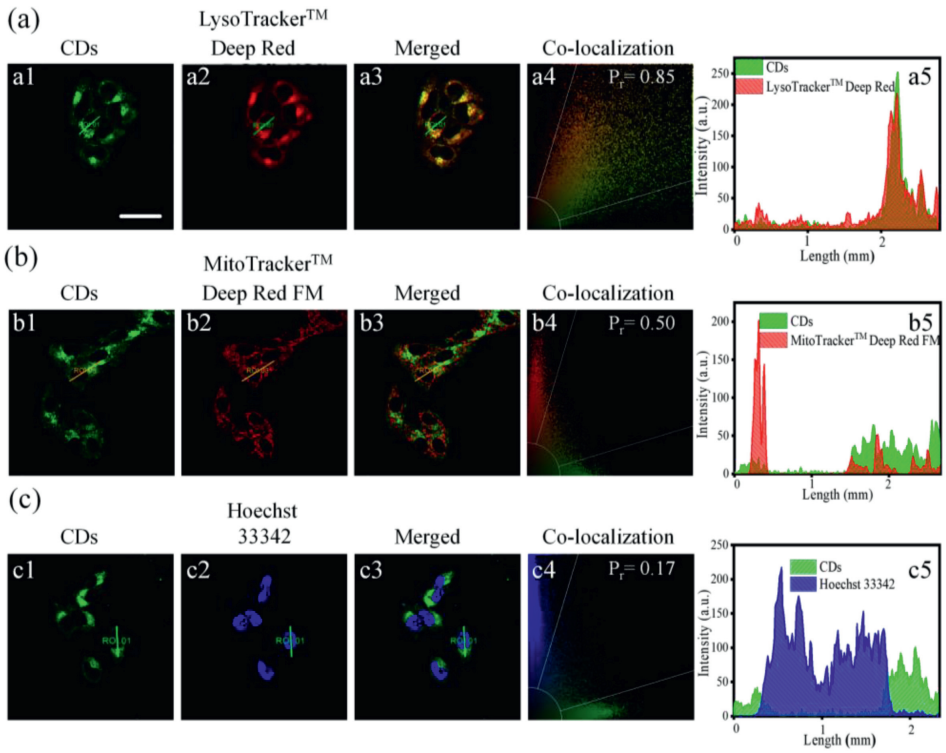

Fig. 2. Confocal fluorescence images, co-localization intensity correlation plots, and fluorescence intensities of the regions of interest in the two channels of HeLa cells co-stained with CDs (50 μg/mL) and commercial probes: (a) LysoTracker™ Deep Red (50 nmol/L), (b) MitoTracker™ Deep Red FM, and (c) Hoechst 33342. λ_{ex} = 405 nm and λ_{em} = 420–480 nm for Hoechst 33342; λ_{ex} = 488 nm and λ_{em} = 500–600 nm for CDs; λ_{ex} = 638 nm and λ_{ex} = 650–750 nm for LysoTracker™ Deep and MitoTracker™ Deep Red FM. Scale bar: 30 μm.

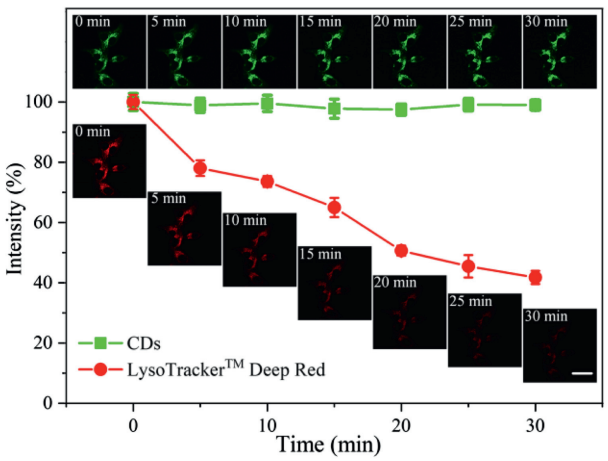

Fig. 3. Photostability comparison of the CDs and LysoTracker™ Deep Red. The error bars represent the mean errors for three cells. Scale bar: 30 μm. Insert pictures: confocal fluorescence images of HeLa cells co-stained with CDs (50 μg/mL) for 20 min and LysoTracker™ Deep Red (50 nmol/L) for 15 min after continuous irradiation for different time periods (λ_{ex} = 488 nm and λ_{em} = 500–600 nm for CDs; λ_{ex} = 638 nm and λ_{em} = 650–750 nm for LysoTracker™ Deep Red).

21.3°, indicating an amorphous structure [37]. The main absorption bands at 3426, 3222, 1743, 1620, 1438, 1295, and 1128 cm^{-1} in the Fourier transform infrared (FTIR) spectrum correspond to the −OH stretching vibration, N−H stretching vibration, −COOH stretching vibration, N−C=O/C=C stretching vibration, B−O stretching vibration, −OH deformation vibration, and C−N/C−O/C−B stretching vibration (Fig. 1c) [22]. The X-ray photoelectron spectroscopy (XPS) spectrum shown in Fig. 1d shows four signals corresponding to B 1s (192.6 eV), C 1s (285.0 eV), N 1s (402.0 eV), and O 1s (532.5 eV) with associated atomic percentages of 6.67%, 65.02%, 2.77%, and 25.53%. The high-resolution XPS spectrum reveals that the B 1s signal consists of two peaks at 192.6 and 192.2 eV, which correspond to B−O and C−B bonds, respectively (Fig. S1 in Supporting information). The C 1s peaks at 284.8, 286.4, and 288.9 eV can be attributed to C−C/C=C/C−B, C−N/C−O, and C=O bonds [38,39]. The N 1s peaks at 400.5 and 402.0 eV represent N−C=O bonds. The O 1s spectrum shows peaks at 532.2 and 533.2 eV, which represent C−O and O−C=O/N−C=O bonds. The zeta potential of the CDs was determined to be −0.81 mV (Fig. S2 in Supporting information), suggesting the potential ability of the CDs to target lysosomes. These characterization results indicate that the CDs were successfully synthesized and functionalized.

The optical properties of the CDs were evaluated based on their fluorescence and UV-vis absorption spectra. As shown in Fig. S3a (Supporting information), the maximum absorption of the CDs is located at 326 nm, corresponding to the π–π^* transition [40]. Under the optimal excitation of 445 nm, the CDs show strong fluorescence at 530 nm with a large Stokes shift of 85 nm. The large Stokes shift indicates the existence of a strong ICT effect in the CDs, in accordance with the design concept mentioned above [36,41-43]. The fluorescence lifetime and quantum yield were determined to be 4.74 ns and 2.9%, respectively (Fig. S3c in Supporting information). In addition, the CDs exhibit good stability and water solubility (Figs. S3b and d in Supporting information).

The fluorescence response of the CDs to polarity was then studied. 1,4-Dioxane with low polarity and water with high polarity have been widely employed to investigate the responsiveness of probes to polarity [44–46]. The fluorescence intensity of the CDs increased as the 1,4-dioxane content in the 1,4-dioxane/water mixture increased, indicating that the CDs showed good polarity responsiveness (Figs. 1e and f). The higher fluorescence in solvents with weaker polarity indicates that the CDs can be ap-

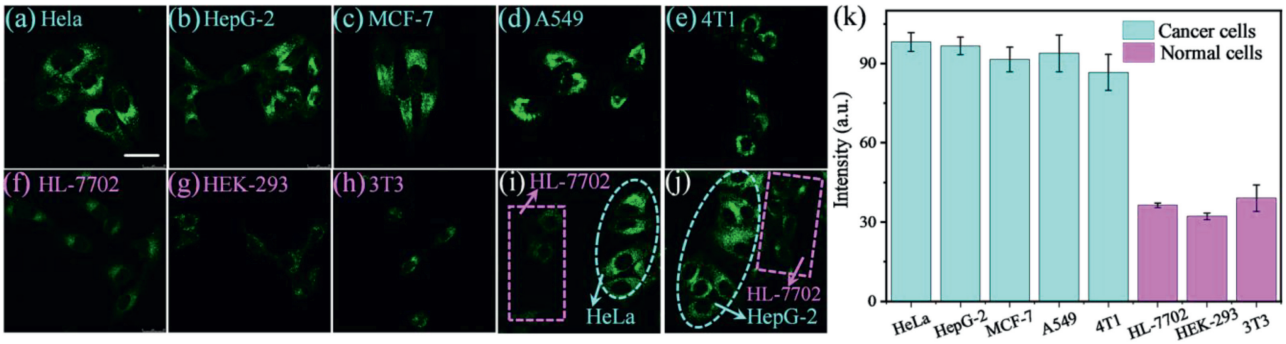

Fig. 4. Confocal fluorescence images of different cells stained with CDs (50 μg/mL) for 20 min: (a) HeLa, (b) HepG-2, (c) MCF-7, (d) A549, (e) 4T1, (f) HL-7702, (g) HEK-293, and (h) 3T3 (λ_{ex} = 488 nm and λ_{em} = 500–600 nm for CDs). Fluorescent images of co-cultured cancer cells (HeLa or HepG-2) and normal cells (HL-7702) stained with CDs: (i) HeLa and HL-7702 cells and (j) HepG-2 and HL-7702. The normal cells and cancer cells are marked by pink rectangles and blue ellipsoids, respectively. Scale bar: 30 μm. (k) Relative fluorescence intensities of different cells.

plied in wash-free imaging because the culture medium and cytoplasm have higher polarities than the lysosomes [47]. Moreover, the polarity of cancer cells is lower than that of normal cells; thus, the CDs may be able to distinguish cancer cells from normal cells. The fluorescence response of the CDs to viscosity was also verified. As shown in Fig. 1g, as the glycerol content or viscosity increases, the fluorescence of the CDs increases obviously (Fig. 1h). Moreover, cancer cells possess higher viscosity than normal cells [31]; thus, the viscosity responsiveness of the CDs lays the foundation for distinguishing between cancer cells and normal cells.

The anti-interference ability of the CDs toward common substances in cells was further examined. The CDs were insensitive to pH in the range of 4 to 8 (Fig. S4 in Supporting information). Upon the addition of various biological species (Fig. S5 in Supporting information) including amino acids (Gly, Thr, Arg, Leu, Met, Pro, Lys, Ala, Try, Iso, His, Asp, Glu, Ser, Val, Cys, Hcy, and GSH), reactive oxygen and nitrogen species (H_2O_2, NO_2^-, OH^-, and ClO^-), and cations (K^+, Na^+, Mg^{2+}, Ca^{2+}, Zn^{2+}, Fe^{2+}, Fe^{3+}, Al^{3+}, Cu^{2+}, Ni^+, and Mn^{2+}), the fluorescence intensity at 530 nm remained almost unchanged, indicating that the CDs have robust anti-interference ability.

The CDs showed good biocompatibility, as determined by CCK-8 cell viability assay (Fig. S6 in Supporting information). The CDs could penetrate living cells rapidly within 5 min, and the optimal incubation time was determined to be 20 min by confocal laser scanning microscopy (Fig. S7 in Supporting information). The optimal incubation concentration of the CDs was determined to be 50 μg/mL (Fig. S8 in Supporting information). Cellular uptake pathway experiments showed that the presence of chlorpromazine (CPZ, the inhibitor of clathrin-mediated endocytosis) significantly reduced the uptake of the CDs, indicating that the CDs entered the living cells through a clathrin-mediated pathway (Fig. S9 in Supporting information). Subsequently, co-localization experiments were conducted to demonstrate the ability of the CDs to selectively accumulate in the lysosomes of living cells. The green fluorescence of the CDs overlapped well with the red fluorescence of LysoTracker™ Deep Red, a commercial lysosome probe, and the Pearson correlation coefficient was calculated to be 85% (Fig. 2). These results demonstrate that the CDs target lysosomes well. In contrast, the Pearson correlation coefficients of the CDs with a commercial mitochondrial probe (MitoTracker™ Deep Red FM) and a commercial nuclear probe (Hoechst 33342) were calculated to be only 50% and 17%, respectively.

Photostability and chemical stability are of great significance in bioimaging as they determine whether a probe can be used for long-term imaging to a large extent. To investigate the photostability of the CDs, HeLa cells were co-stained with CDs and LysoTracker™ Deep Red, and the fluorescence intensity of the two channels was evaluated after continuous laser irradiation for 30 min. The fluorescence of the CDs remained stable (Fig. 3), indicating that the CDs have good stability. In contrast, the fluorescence intensity of LysoTracker™ Deep Red decreased by nearly 60% during the 30 min of continuous irradiation. After incubation with HeLa cells for 48 h, the CDs exhibited strong fluorescence, suggesting that the CDs have excellent chemical stability, which can be applied in long-term lysosomal imaging (Fig. S10 in Supporting information). Additionally, the CDs showed great potential for wash-free imaging. As shown in Fig. S11 (Supporting information), no obvious background fluorescence can be observed in the culture medium and cytoplasm without any washing. The ability of the CDs to be applied in wash-free imaging can be attributed to their polarity- and viscosity-responsiveness [38].

Taking advantage of the responsiveness of the CDs to polarity and viscosity, the CDs were used to differentiate normal cells from cancer cells by fluorescence imaging. Five types of cancer cells (HeLa, HepG-2, MCF-7, A549, and 4T1) and three types of normal cells (HL-7702, 3T3, and HKE-293) were tested. As shown in Fig. 4, the cancer cells stained with CDs exhibit stronger fluorescence (Figs. 4a–e) than the normal cells with high contrast (Figs. 4f–h). Therefore, the CDs can successfully distinguish a broad spectrum of cancer cells from normal cells without any other chemical treatment [5].

Cancer cells (HeLa and HepG-2) and normal cells (HL-7702) were also co-cultured with CDs [48]. As shown in Fig. 4i, HeLa and HL-7702 cells were seeded in the same dish and incubated for 24 h. After being treated with CDs (50 μg/mL) for 20 min, bright fluorescence was observed in the HeLa cells, whereas the HL-7702 cells emitted negligible fluorescence. Similarly, HepG-2 cells showed brighter fluorescence than HL-7702 cells (Fig. 4j). These results demonstrate that the developed lysosome-targeting dual microenvironment-responsive CDs can accurately distinguish cancer cells from normal cells.

In summary, we have developed a new kind of lysosome-targeting CDs with dual response to polarity and viscosity through facile synthesis for the fluorescence-based diagnosis of a broad spectrum of cancer cells with high contrast. The CDs exhibit many advantages including good water solubility, pH-independent emission, wash-free imaging ability, good biocompatibility, and excellent photostability, which can differentiate cancer cells from normal cells based on the lower polarity and higher viscosity of the lysosome microenvironment in cancer cells. The CDs are promising candidates for application in the field of cancer diagnosis, and the design strategy based on the response of cellular organelle-

targeting CDs to multiple environmental parameters is expected to inspire more studies in this research field.

Declaration of competing interest

The authors declare that they have no known competing financial interests or personal relationships that could have appeared to influence the work reported in this paper.

Acknowledgments

This work was supported by the National Natural Science Foundation of China (Nos. 21974125, 21708035), Program for Innovative Research Team (in Science and Technology) in University of Henan Province (No. 22TRTSTHN002), the 111 Project of Henan Province (No. CXJD2021001) and National 111 Project (No. D20003).

Supplementary materials

Supplementary material associated with this article can be found, in the online version, at doi:10.1016/j.cclet.2022.03.109.

References

[1] R.L. Siegel, K.D. Miller, H.E. Fuchs, A. Jemal, Ca-Cancer J. Clin. 71 (2021) 7–33.
[2] Y. Zhou, G.A. Abel, W. Hamilton, et al., Nat. Rev. Clin. Oncol. 14 (2017) 45–56.
[3] J.V. Frangioni, J. Clin. Oncol. 26 (2008) 4012–4021.
[4] J. Liu, H. Meng, L. Zhang, et al., Chin. Chem. Lett. 32 (2021) 3421–3425.
[5] J. Liu, M. Liu, H. Zhang, W. Guo, Angew. Chem. Int. Ed. 60 (2021) 12992–12998.
[6] Y. Cheng, G. Shabir, X. Li, et al., Chem. Commun. 56 (2020) 1070–1073.
[7] Z. She, W. Wang, G. Mao, et al., Chem. Commun. 57 (2021) 4811–4814.
[8] X. Wu, R. Wang, S. Qi, et al., Angew. Chem. Int. Ed. 60 (2021) 15418–15425.
[9] B. Wang, S. Lu, Matter 5 (2022) 110–149.
[10] Z. Zhu, Y. Zhai, Z. Li, et al., Mater. Today 30 (2019) 52–79.
[11] C. Xia, S. Zhu, T. Feng, et al., Adv. Sci. 6 (2019) 1901316.
[12] D. He, M. Yan, P. Sun, et al., Chin. Chem. Lett. 32 (2021) 2994–3006.
[13] X. Hu, S. Wang, Q. Luo, et al., Chin. Chem. Lett. 32 (2021) 2287–2291.
[14] X. Geng, Y. Sun, Z. Li, et al., Small 15 (2019) 1970259.
[15] B. Wang, J. Yu, L. Sui, et al., Adv. Sci. 8 (2021) 2001453.
[16] X. Yang, L. Sui, B. Wang, et al., Sci. China Chem. 64 (2021) 1547–1553.
[17] W. Li, Y. Liu, B. Wang, et al., Chin. Chem. Lett. 30 (2019) 2323–2327.
[18] X. Shi, H. Meng, Y. Sun, et al., Small 15 (2019) 19011507.
[19] Z. Lei, L. Ding, C. Yao, et al., Adv. Mater. 31 (2019) 1807456.
[20] J. Li, S. Yang, Z. Liu, et al., Adv. Mater. 33 (2021) 2005096.
[21] Q. Zhang, S. Deng, J. Liu, et al., Adv. Funct. Mater. 29 (2019) 1805860.
[22] S. Li, W. Su, H. Wu, et al., Nat. Biomed. Eng. 4 (2020) 704–716.
[23] S.M. Usama, K. Burgess, Acc. Chem. Res. 54 (2021) 2121–2131.
[24] Z. Yang, J. Cao, Y. He, et al., Chem. Soc. Rev. 43 (2014) 4563–4601.
[25] Y. Song, H. Zhang, X. Wang, et al., Anal. Chem. 93 (2021) 1786–1791.
[26] X. Liu, X. Gong, J. Yuan, et al., Anal. Chem. 93 (2021) 5420–5429.
[27] W. Xu, Z. Zeng, J.H. Jiang, et al., Angew. Chem. Int. Ed. 55 (2016) 13658–13699.
[28] S.J. Park, V. Juvekar, J.H. Jo, H.M. Kim, Chem. Sci. 11 (2020) 596–601.
[29] H. Izumi, T. Torigoe, H. Ishiguchi, et al., Cancer Treat. Rev. 29 (2003) 541–549.
[30] L. Fan, X. Wang, J. Ge, et al., Chem. Commun. 55 (2019) 4703–4706.
[31] R. Chowdhury, A. Saha, A.K. Mandal, et al., J. Phys. Chem. B 119 (2015) 2149–2156.
[32] Z. Liu, W. He, Z. Guo, Chem. Soc. Rev. 42 (2013) 1568–1600.
[33] N. Jiang, J. Fan, F. Xu, et al., Angew. Chem. Int. Ed. 54 (2015) 2510–2514.
[34] Y. Sun, H. Qin, X. Geng, et al., ACS Appl. Mater. Interfaces 12 (2020) 31738–31744.
[35] H. Liu, J. Yang, Z. Li, et al., Anal. Chem. 91 (2019) 9259–9265.
[36] K. Xin, X. Li, Y. Guo, et al., CCS Chem. 2 (2020) 2307–2315.
[37] G. Han, J. Zhao, R. Zhang, et al., Angew. Chem. Int. Ed. 58 (2019) 7087–7091.
[38] P. Gao, J. Wang, M. Zheng, Z. Xie, Chem. Eng. J. 381 (2020) 122665.
[39] S. Chen, Y. Jia, G.Y. Zou, et al., Nanoscale 11 (2019) 6377–6383.
[40] H. Singh, S. Sreedharan, K. Tiwari, et al., Chem. Commun. 55 (2019) 521–524.
[41] T.B. Ren, W. Xu, W. Zhang, et al., J. Am. Chem. Soc. 140 (2018) 7716–7722.
[42] A. Dhara, T. Sadhukhan, E.G. Sheetz, et al., J. Am. Chem. Soc. 142 (2020) 12167–12180.
[43] L. He, H. Xiong, B. Wang, et al., Anal. Chem. 92 (2020) 11029–11034.
[44] A. Jimenez-Sanchez, E.K. Lei, S.O. Kelley, Angew. Chem. Int. Ed. 57 (2018) 8891–8895.
[45] X. Li, X. Li, H. Ma, Chem. Sci. 11 (2020) 1617–1622.
[46] T.C. Owyong, P. Subedi, J. Deng, et al., Angew. Chem. Int. Ed. 59 (2020) 10129–10135.
[47] H. Qin, Y. Sun, X. Geng, et al., Anal. Chim. Acta 1106 (2020) 207–215.
[48] G. Gao, Y. Jiang, J. Yang, F. Wu, Nanoscale 9 (2017) 18368–18378.